Heliyon 10 (2024) e27538

Contents lists available at ScienceDirect

Heliyon

journal homepage: www.cell.com/heliyon

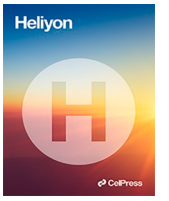

Research article

Crystallinity as a factor of SERS stability of silver nanoparticles formed by Ar^+ irradiation

Natalia V. Doroshina [a], Oleg A. Streletskiy [b], Ilya A. Zavidovskiy [a], Mikhail K. Tatmyshevskiy [a], Gleb I. Tselikov [c], Olesya O. Kapitanova [a,d], Alexander V. Syuy [a], Roman Romanov [a], Prabhash Mishra [e], Vjaceslavs Bobrovs [f], Andrey M. Markeev [a], Dmitry I. Yakubovsky [a], Irina A. Veselova [d], Aleksey V. Arsenin [a,g], Valentyn S. Volkov [c,g], Sergey M. Novikov [a,*]

[a] *Moscow Center for Advanced Studies, Kulakova Str. 20, Moscow, Russia*
[b] *Faculty of Physics, M.V. Lomonosov Moscow State University, 119991, Moscow, Russia*
[c] *Emerging Technologies Research Center, XPANCEO, Dubai, 00000, United Arab Emirates*
[d] *Faculty of Chemistry, M.V. Lomonosov Moscow State University, 119991, Moscow, Russia*
[e] *Quantum Materials and Devices Laboratory, Faculty of Engineering and Technology, Jamia Millia Islamia (Central University), 110025, New Delhi, India*
[f] *Institute of Photonics, Electronics and Telecommunications, Riga, 1048, Latvia*
[g] *Yerevan State University, 0025, Yerevan, Armenia*

ARTICLE INFO

Keywords:
Plasmonics
SERS
Monocrystalline silver nanoparticles
Low-energy Ar^+ irradiation
Metal optics
Linear spectroscopy

ABSTRACT

The plasmonic sensors based on silver nanoparticles are limited in application due to their relatively fast degradation in the ambient atmosphere. The technology of ion-beam modification for the creation of monocrystalline silver nanoparticles (NPs) with stable plasmonic properties will expand the application of silver nanostructures. In the present study, highly-stable monocrystalline NPs were formed on the basis of a thin silver film by low-energy ion irradiation. Combined with lithography, this technique allows the creation of nanoparticle ensembles in variant forms. The characterization of the nanoparticles formed by ion-beam modification showed long-term outstanding for Ag nanoparticles stability of their plasmonic properties due to their monocrystalline structure. According to optical spectroscopy data, the reliable plasmonic properties in the ambient atmosphere are preserved for up to 39 days. The mapping of crystal violet dye via surface-enhanced Raman spectroscopy (SERS) revealed a strong amplification factor sustaining at least thrice as long as the one of similarly sized polycrystalline silver NPs formed by annealing. The plasmonic properties sustain more than a month of storage in the ambient atmosphere. Thus, ion-beam modification of silver film makes it possible to fabricate NPs with stable plasmonic properties and form clusters of NPs for sensor technology and SERS applications.

* Corresponding author.
E-mail address: novikov.s@mipt.ru (S.M. Novikov).

https://doi.org/10.1016/j.heliyon.2024.e27538
Received 4 December 2023; Received in revised form 20 February 2024; Accepted 1 March 2024
Available online 9 March 2024

1. Introduction

The interaction of metal nanostructures with light has become the subject of lots of research due to its efficiency and breadth of application [1–3]. One of the remarkable results of such interaction is a field enhancement (FE) effect arising due to the resonant excitation of collective electron oscillations, i.e., so-called localized surface plasmons (LSPs) [4–6]. The FE effect finds wide application, particularly in optics, electronics, catalysis and a diverse family of sensors [3–6]. One of the important directions in sensorics is based on the surface-enhanced Raman scattering (SERS) effect [6–10]. SERS is a highly sensitive (detecting the order of nM concentrations) and selective tool for chemical identification and determination of the structure of molecules and materials, based on their specific vibrational coupling [10–13]. For the SERS application, it is particularly important that reliable and controllable FE is achieved by competently chosen nanostructures and the stability of their plasmonic properties. Among the noble metals used for SERS nanostructures, copper, gold and silver are the mainly used ones, due to their plasmon resonance in the visible region [12,14–16]. Among the mentioned plasmonic-active metals, silver has excellent plasmonic properties and can be beneficially applied not only in SERS but also in the other areas mentioned above [14,15,17]. The techniques widely used for the formation of silver plasmonic structures are: sputtering or evaporation, photoreduction, chemical synthesis, etc. [17–20]. Despite the abundance of methods for the fabrication of silver structures, the rapid oxidation or sulfidation of silver in the ambient atmosphere leads to the decreasing plasmonic efficiency of the material and causes many difficulties in its practical application [21,22]. As a way to overcome these limitations, protective layering on the surface of the silver nanostructures can be formed to prevent the degradation influence of the environment [23,24]. Nevertheless, such an approach is not a universal tool due to the complexity of production. One of the ways to improve the oxidation resistance and maintain the high stability of plasmonic properties of silver nanoparticles (NPs) can be the formation of the NPs with monocrystalline structure. Earlier research showed, that monocrystalline structure might be more stable than polycrystalline one [25]. This effect may originate from the preferential oxidation of the grain boundaries, which is more prominent for polycrystalline particles. An efficient way to obtain NPs is the fabrication of pure particles with perfect crystalline structure by aggregation of metal atoms into clusters from very pure sources in a vacuum [26–28]. Such particles can be aggregated into beams, size-selected, and deposited or implanted inside or on top of different substrates, providing a great capability to control the structure and properties of materials on the nanoscale [26,29]. This method is excellent for nanostructuring large areas but there are some issues in the case of the formation of more complex surfaces. In this work, we present a more flexible method allowing the formation of NPs and nanostructuring of substrates. Magnetron deposition of continuous silver film and its subsequent ion beam irradiation make it possible to create silver NPs with pure monocrystalline structure. This method allows us to nanostructure large areas and control such parameters as size and coverage density of NPs [30]. The combination of this technique with electron-beam lithography allows the creation of various sophisticated combinations of nanostructuring surfaces. In this investigation, we study the effectiveness of single-crystal silver nanoparticles. We utilize a manufacturing technique based on magnetron sputtering and low-energy ion irradiation as a method of fabricating ensembles of monocrystalline Ag NPs with controlled sizes. Ag NPs of about 15–20 nm were formed on silicon and glass substrates. In order to compare the influence of the monocrystal nature of nanoparticles on the stability of their plasmonic properties, we created a series of polycrystalline Ag NPs by annealing the silver layer deposited by magnetron on a glass substrate [31,32]. The formed nanoparticles were characterized by Scanning Electron Microscopy (SEM), Transmission Electron Microscopy (TEM), linear spectroscopy, Raman and X-ray photoelectron spectroscopy (XPS) analyses. The monocrystalline NPs demonstrate a strong FE and a stable plasmon band intensity, which decreases by about 10% in a long-term period of 39 days at room temperature in the ambient atmosphere. The comparison of the results of the characterization of monocrystalline and polycrystalline silver nanoparticles shows a clear advantage of the single-crystal structure due to its stability of plasmonic properties. Thus, in this work, we demonstrate a method of silver NPs fabrication with stable plasmonic properties, that can be used on an industrial scale due to large production volumes and high reproducibility of stable properties of nanoparticles. We suppose the presented results to be useful for the development of sensor applications of silver.

2. Methods

2.1. Ag NPs by ion-beam modification of Ag film

For the manufacturing of silver NPs by the ion-beam irradiation method, silicon and cover glass were used as substrates. The surface of the substrates was preliminarily prepared by ion beam etching for 5 min in a high-vacuum chamber. For the irradiation, Ar^+ ions with the energy of 1 keV were generated by a Hall-type ion beam source Klan 53-M with cold hollow cathode (Platar Corp.). The irradiation dose of 5×10^{14} ion/cm^2 ensured a negligible morphology variation of the Si substrates during the etching [33,34]. Then thin silver films were deposited by radio-frequency magnetron sputtering. Before the coating process, the chamber was evacuated to 10^{-5} torr, after which synthesis took place in an argon atmosphere at the pressure of 8×10^{-4} torr. Using a radio-frequency magnetron with a power of about 30 W and a silver target of 99.99% purity, a thin film of silver was deposited. The thickness of silver films obtained in this way was about ~25 nm, based on the measurements of the quartz oscillator (Inficon Corp.). Next, an ion beam source based on the Hall effect was used to form the NPs on the resulting films. The silver-coated substrates were irradiated with argon ions with the energy of 150 eV and the dose of 4.5×10^{16} ion/cm^2. During the film deposition and irradiation, the angle between the Ag/Ar^+ flux and the substrate surface was 45°. Such deposition parameters ensured low damage of the substrate and prominent SERS performance of the Ag NPs. Electron-beam lithography (Quanta 3D FEI with Ga ion source) was used to create the ensembles of silver particles with nanodisks shape of 25 nm height and ~500 nm diameter. The subsequent ion irradiation allowed converting each disk to the group of spheroidal NPs of about 18–27 nm localized within the boundaries of the previously continuous disk. The fabrication

process is shown schematically in Fig. 1. This fabrication method makes it possible to nanostructure the surface with clusters of nanoparticles, adjusting their size [30]. Additionally, for the time dependence measurements, by the method mentioned above, but without e-beam lithography, ten identical samples with Ag NPs on the glass substrate were prepared in one cycle.

2.2. Ag NPs by annealing technique

The ultra-thin Ag films with the 7 nm thickness were deposited in one regime by electron beam evaporation in a Nano Master NEE-4000 (NANO-MASTER Inc., Austin, TX, USA) installation at a high vacuum, with the pressure of residual gasses in the chamber being no greater than 5×10^{-6} torr and deposition rate of 0.5 Å/s at room temperature (21 °C). Before the deposition, the glass slides were cleaned from organic pollutants with a piranha solution, a mixture of sulphuric acid (H_2SO_4) and hydrogen peroxide (H_2O_2) in a ratio of 3:1 to 7:1. Then glass substrates were then extensively rinsed with deionized water. Then the surface of the samples was cleaned by oxygen plasma treatment (Microsensor LLC). The granulated target of Ag with a purity of 99.999% was produced by Kurt J. Lesker (East Sussex, UK). During the deposition, the thickness of Ag films was controlled by the quartz oscillator mass-thickness sensor. After the deposition, the glass substrates with Ag films were immediately annealed to avoid oxidation or sulphidisation processes. High-temperature annealing was carried out in a CVD Oxford PlasmaLab 100 chamber with the ability to provide a pressure of 10^{-5} torr during annealing at the temperature of 300 °C for 2 h. The range of the diameters of obtained particles was 10–35 nm.

2.3. Linear spectroscopy and Raman characterization

A UV–Vis–NIR spectrophotometer Agilent Technologies Cary 5000 (175–3300 nm) was used to analyze the optical properties of the obtained nanoparticles. The experimental setup used for SERS measurements was a confocal scanning Raman microscope Horiba LabRAM HR Evolution (HORIBA Ltd., Kyoto, Japan). All the measurements were carried out using linearly polarized excitation at the wavelength of 532 nm, the 600 lines/mm diffraction grating, and × 100 objective (N.A. = 0.90). The spot size was ~0.4 μm. The Raman spectra were recorded with 0.05 mW incident powers and the integration time of 1 and 3 s at each selected point. The statistics collected at least 10 points for each sample.

2.4. XPS characterization

The measurements were performed by the Theta Probe (Thermo Scientific, Walthamm, MA, USA) system with a monochromatic Al Ka (1486.6 eV) X-ray source. The photoelectron spectra were acquired in the fixed analyzer transmission mode with the pass energy of 50 eV. For the detailed study of the fabricated NPs, we carried out the angle-dependent measurements of the O1s and C1s core level XPS spectra. In order to investigate the contributions of different bonds, the Ag3d core-level spectra were fitted using the MagicPlot software package.

2.5. Microscopy techniques

The roughness and homogeneity of the substrate were measured by an atomic force microscope (NT-MDT Ntegra, Moscow, Russia). The visualization of fabricated NPs was done by the scanning electron microscope using the acceleration voltage of 3 kV (JEOL JSM-7001F, Tokyo, Japan) and Transmission Electron Microscopy (TEM, Jeol JEM-2100, Japan) equipped with the 200 kV field emission gun and the point resolution of 0.19 nm.

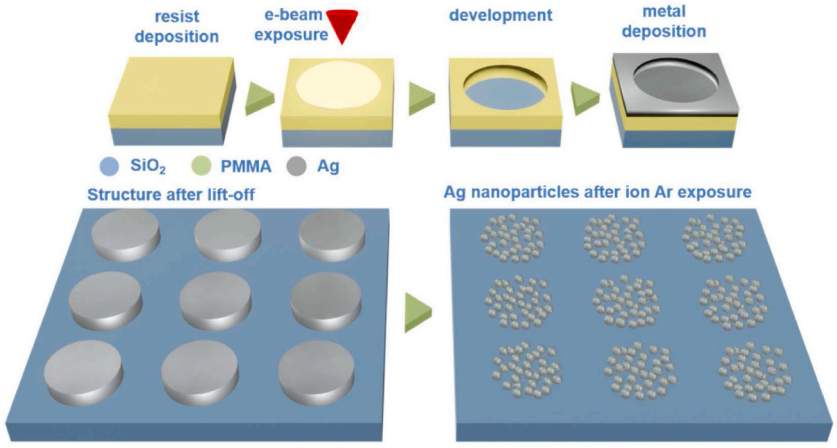

Fig. 1. Schematic illustration of the fabrication procedure.

3. Results and discussion

We fabricated the periodic nanostructure consisting of the Ag discs with diameter of 500 nm, a height of 25 nm and a period of 1 μm (see Methods) atop a Si substrate using electron beam lithography. By argon irradiation of continuous Ag discs, NPs of fixed sizes and surface distributions were formed. The schematic illustration of the fabrication procedure is shown in Fig. 1.

SEM images (Fig. 2a and b) show the high quality of the fabricated samples. The combination of SEM and AFM analysis demonstrated that the formed NPs are tightly packed within the discs' borders, formed by lithography, featuring a height of about 23 nm (Fig. 2 b,e). An ethanol solution of Crystal Violet (CV) with a concentration of 10^{-6} M was layered by drop casting to the formed disks consisting of Ag NPs to make sure the fabricated structure retained its original shape after the interaction with the liquid. The SERS images of the samples show that the Ag NPs formed by the ion-beam method keep their shape well within the boundaries of the initial structures irradiated by lithography (Fig. 2c–f). The signal at the 443 cm^{-1} was selected as a well-resolved CV characteristic band for SERS spectra and maps (Fig. S1). Previously, we showed that various thicknesses of precursor Ag film, as well as various ion irradiation doses, make it possible to deposit the structures with different morphologies [30]. We demonstrated at the precursor film thickness of 20–30 nm the distribution of the Ag NPs is determined by the sputtering and resputtering of the unfavorably-oriented crystallites and amorphous fragments [30].

That allowed us to assume that the NPs deposited at the suggested parameters have a good crystallinity, known to be beneficial for their plasmonic stability [25]. In order to confirm this, as well as to check the stability of the obtained nanoparticles and therefore their applicability for sensors, a detailed time-resolved characterization of the particles was carried out using several complementary methods. For this investigation, we prepared 10 identical samples consisting of the NPs obtained by ion beam irradiation and formed on the glass substrate in one cycle (see Methods). The SEM images (Fig. 3 a,b) show the 25-nm-thick Ag film deposited on a glass substrate before, and the Ag NPs formed from this film after ion beam irradiation. Further TEM analysis demonstrated, that the formed Ag NPs have a monocrystalline structure (Fig. 3c) with a face-centered cubic lattice of bulk Ag [35]. The microscopy revealed that the vast majority of the NPs formed by ion irradiation were monocrystalline, and only a slight amount (less than 5%) of polycrystalline particles was observed. In order to verify, how long single crystal NPs can hold their structure, we performed a detailed TEM analysis of the manufactured nanoparticles on the day of fabrication, 14 days later and 26 days later consequently. The results of the analysis showed that the nanoparticles hold their single-crystal structure (Figure SI 1b,c). The stability of plasmonic properties was examined by linear spectroscopy. The characterization of the monocrystalline nanoparticles was carried out within 39 days (Fig. 4a). The localized surface plasmon resonance (LSPR) band with the maximum intensity of about 418 nm is visible on the spectra on the day of fabrication.

After 7 days the resonance band starts shifting to the red region, and the intensity also begins decreasing and keeps doing it until day 23 of measurements. After 39 days of measurements, the peak position moved to 425 nm and the intensity decreased by less than 10%, indicating the plasmonic efficiency of the nanostructures and the stability of the optical properties of the nanoparticles. Additionally, we made the X-ray photoelectron spectroscopy (XPS) analysis (Fig. 4 b, Figure SI 4a).

In the case of oxidation, the Ag3d peaks are expected to shift to the lower energy region [36,37]. The spectra measured from the NPs

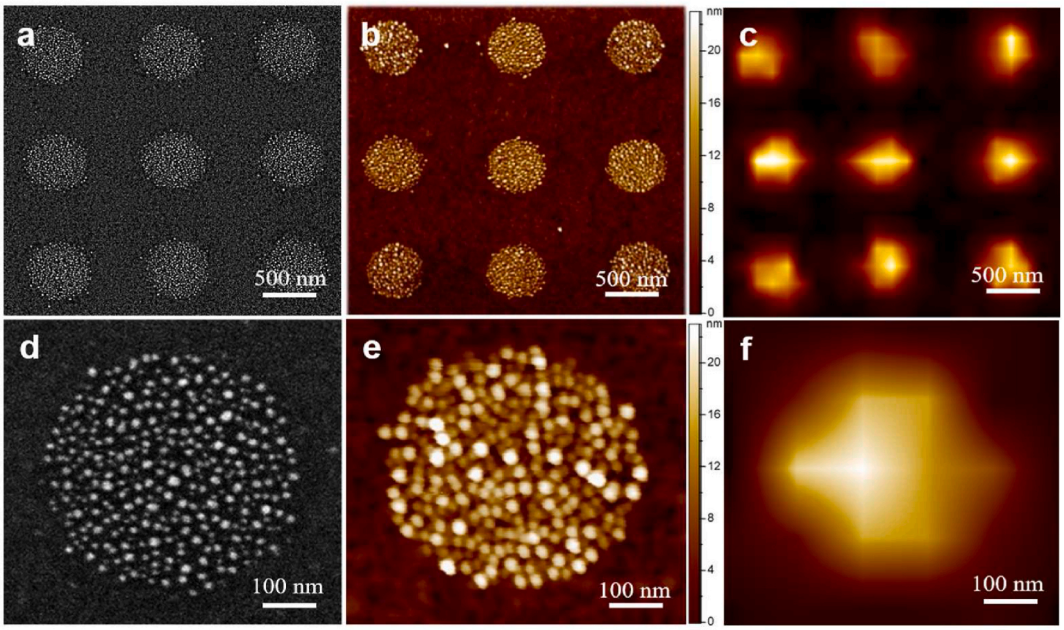

Fig. 2. SEM images (a,d), AFM images (b,e), and SERS images (c,f) of silver NPs obtained by the combination of lithography and by low-energy ion beam irradiation.

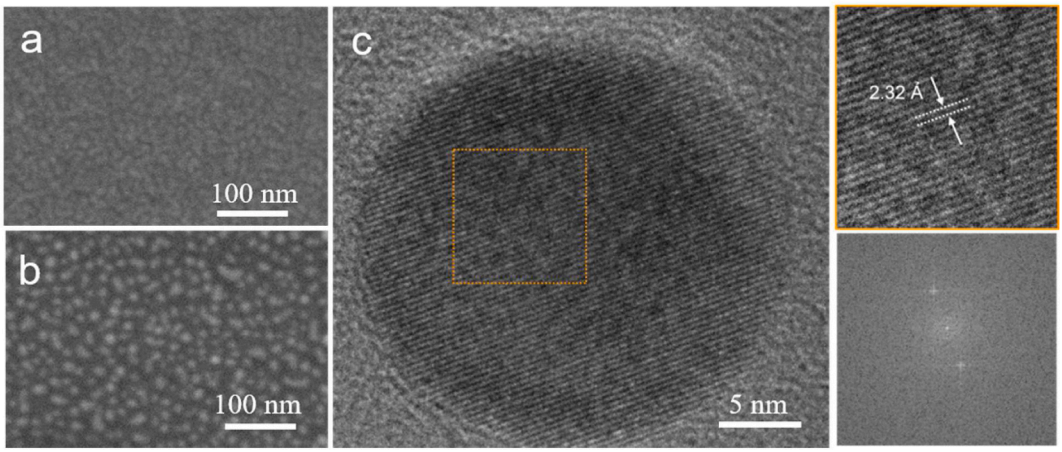

Fig. 3. SEM images of a) Ag film with the thickness of 20 nm b) Ag NPs formed by low-energy Ion Beam Irradiation; c) TEM image of the 23-nm-sized silver NPs with a corresponding high-resolution TEM (top-right subfigure) demonstrating (111) atomic planes of face-centered cubic structure and fast Fourier plot (bottom-right subfigure).

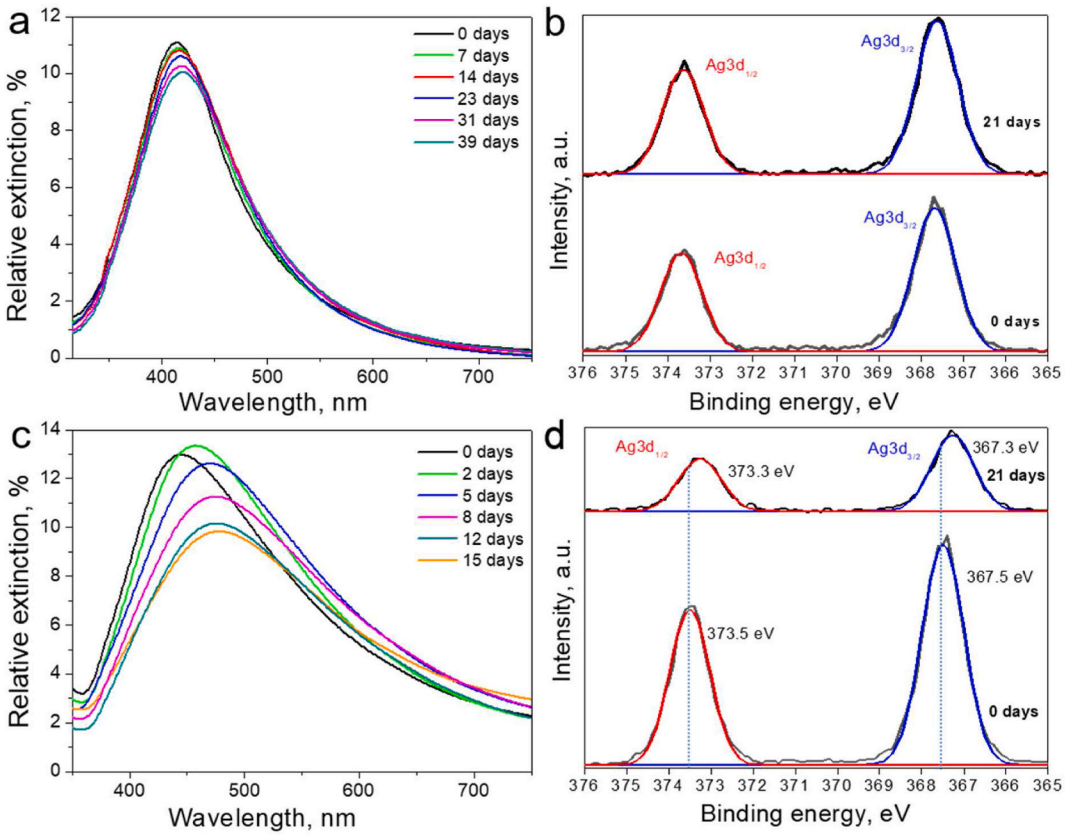

Fig. 4. a) Experimental extinction spectra of the Ag NPs formed by low-energy ion beam irradiation, as a function of time. b) XPS spectra of the Ag NPs obtained on the day of fabrication and 21 days later. c) Experimental extinction spectra of Ag NPs formed by annealing process, as a function of time. d) XPS spectra of annealed Ag NPs obtained on the day of fabrication and after 21 days.

on the day of fabrication and 21 days later do not show any reliably distinguished changes in the peaks' position (Fig. 4b). The appearance of a slight red shift is probably caused by the formation of an oxide shell on the NPs, due to the interaction with the environment.

In order to demonstrate that the monocrystalline structure is the factor responsible for the prolonged stability of plasmonic

properties of Ag NPs, the other sets of Ag NPs were created using the annealing method, which has long been well-known [31] and ensures simple nanostructuring of the selected surface with spheroidal nanoparticles (Fig. 5a). This simple method makes it possible to control the distribution density and the size of NPs by the variation of the annealing time, the temperature, and the thickness of precursor thin films [31]. Ultrathin silver films of 7 nm were deposited on glass substrates and were subsequently annealed in a vacuum furnace at 300 °C for 3 h (see Methods). The fabrication parameters were selected to obtain particles with sizes and distribution close to the Ag NPs obtained by the method of ion-beam modification (Figs. 5b,c, SI 2,3). Ten identical samples were prepared in one cycle of fabrication and were examined using the same procedure as Ag NPs fabricated by ion-beam modification.

The SEM images (Fig. 5c) show formed NPs on the glass substrate. The NPs formed by the annealing method have a mainly spheroidal shape and diameter varying from 10 to 35 nm, while the diameters of the NPs formed by ion-beam irradiation mostly fall within the range of 6–22 nm.

The analysis of the TEM images show that the NPs formed by the annealing method preferentially have a polycrystalline structure (Fig. 5c and d, Figure SI 2) but at least 15–20% of the particles have a single crystal structure (Figure SI 4a). As in the case of the NPs formed by the ion-beam irradiation method, the TEM characterization for the annealed NPs was performed on the day of fabrication, 14 and 26 days later (Figure SI 2, SI 4b). The images illustrate, that even after 14 days the polycrystalline NPs do not show a clear structure due to their oxidation and after 26 days any structure features disappear completely (Figure SI 2c). At the same time, the nanoparticles having a single-crystal structure perfectly preserve it (Figure SI 4b). The intensity and spectral position of the plasmon band of annealed Ag NPs were monitored for 15 days (Figure SI 5a). The extinction spectrum recorded on the day of fabrication shows a wide LSPR band with the maximum at about 450 nm. The broad shape can be explained by the distribution of sizes and non-ideal spheroidal shape of the annealed NPs.

After 2 days, the resonance becomes red-shifted with the intensity slightly increased, which can be probably explained by the deformation of the shape of the particles from a spheroidal shape to an ellipsoidal one [25]. Then the intensity of the resonance band continues red-shifting while starting to broaden, and its intensity decreases. After 15 days the resonance intensity decreases by nearly 40%. As SPR peak intensity is known to be considerably affected by the oxidation of silver nanoparticles [37], the dynamics of its change confirm that AgNPs produced by annealing deteriorate significantly faster than ion-irradiated AgNPs. However, due to the presence of stable single-crystal particles in the ensembles of annealed NPs, the resonance does not completely disappear when the majority of the particles are oxidized. To confirm that plasmonic properties degradation is related to oxide layer formation, we

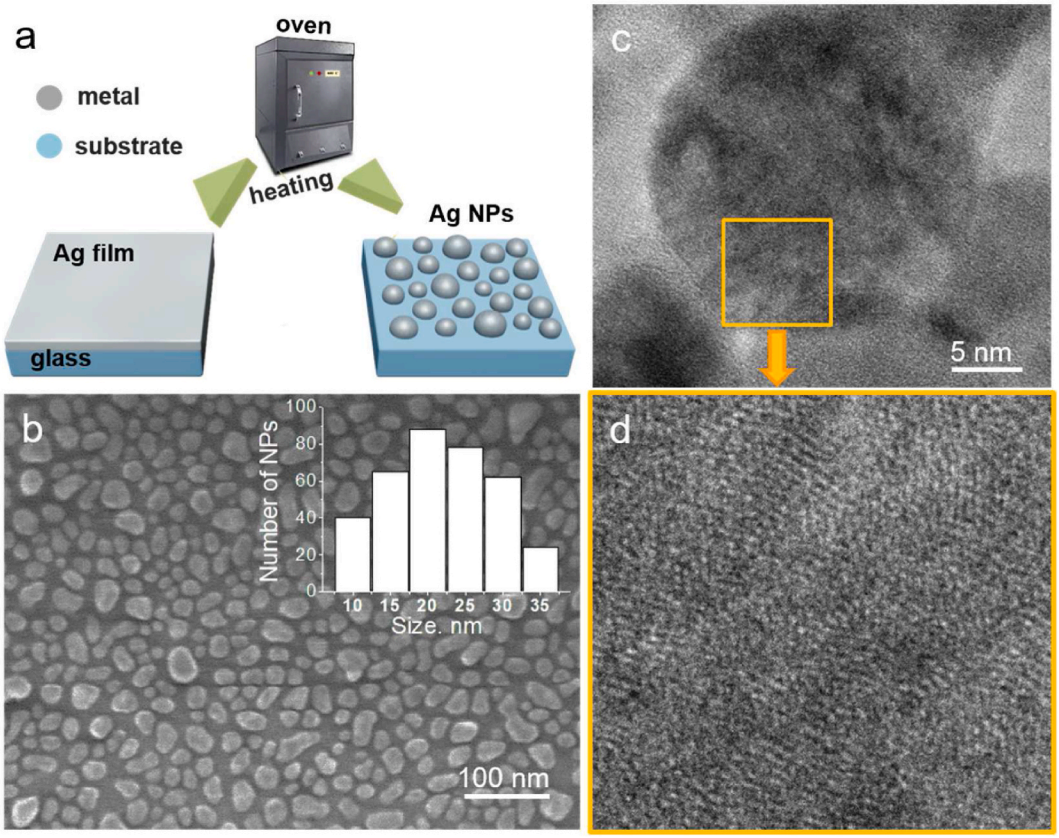

Fig. 5. a) Schematic illustration of the annealing method, b) SEM image of the Ag NPs formed by the annealing method, c) TEM image of the 22-nm-sized Ag NPs d) high-resolution TEM image from the area marked on b) by yellow color. The inset of Figure (b) demonstrates the distribution of NPs' sizes. (For interpretation of the references to color in this figure legend, the reader is referred to the Web version of this article.)

examined the annealed NPs by XPS analysis, similar to the one performed for the NPs obtained by the ion beam irradiation method (Figs. 4d and SI 5b). The XPS spectra recorded after 15 days show that the Ag 3d peak has a negative shift of about 0.3–0.4 eV (Figure SI 5a), which can be associated with the oxidation of the NPs [37,38]. The results obtained by XPS, have a good agreement with the ones obtained by TEM and linear spectroscopy.

Finally, the Ag NPs batches formed by both methods were characterized by SERS. The SERS signal intensity is well known to decrease during silver oxidation [37], so the enhancement factor of signal intensity can be used as a marker of the stability of the fabricated particles. For SERS measurements, one sample was selected from each batch of annealed samples and the other ones obtained by ion-beam modification and was coated with ethanol Crystal Violet (CV) dye solution with concentration of 10^{-6} M and dried out for nearly 10 min each. A similar procedure was repeated on each day selected for new measurements. Typical SERS spectra, of monocrystalline Ag NPs obtained by ion-beam modification (Fig. 6a), show high stability. After the NPs fabrication, the intensity of the SERS signal slightly decreases, with time, and after 39 days, the intensity decreased by nearly~7–10% (Fig. 6 a,b, Figure SI 6a).

On the contrary, the intensity of the SERS spectra obtained from the annealed NPs demonstrates a dramatic intensity decrease even after 5 days and by the day 15 the intensity almost halved (Fig. 6c and d, Figure SI 6b). For more clarity, we plotted the dependence of the intensity on the days after the NPs manufacturing by both methods (Fig. 6b–d). The variation of SPR deterioration dynamics (Fig. 4a, c) and drastic variation in the longevity of the SERS performance of investigated samples (Fig. 6b, d) confirm that the stability of the plasmonic properties of the nanoparticles considerably depends on their oxidation resistance, and, hence, on their crystallinity.

One prominent difference between the SERS spectra of annealed and ion-irradiated samples is a relative intensity decrease of the 1370-cm^{-1}-centered line for the spectra of the CV adsorbed to the AgNPs produced by annealing. Peak located in the vicinity of 1370 cm-1 can be attributed to nitrogen-phenyl stretching [39]. As nitrogen atoms are located at the edges of CV molecules, the variation of ~1370 cm^{-1} intensity can be caused by various CV-AgNP bonding which can be due to the difference in AgNPs' crystallinity, distribution and oxidation degree.

To quantify the plasmonic performance of the investigated AgNPs, we calculated the enhancement factor (EF) for the fabricated NPs using an analytical enhancement factor expression (1) which quantifies how much more signal can be expected from SERS compared to the conventional Raman spectroscopy with the same experimental parameters [40]. The average EF is determined by comparing the signals recorded from the CV at the concentration of 10^{-2} M deposited on an uncoated glass, with the signals obtained with the concentration 10^{-6} M of the CV deposited on the glass substrates with the Ag NPs formed by annealing and ion beam

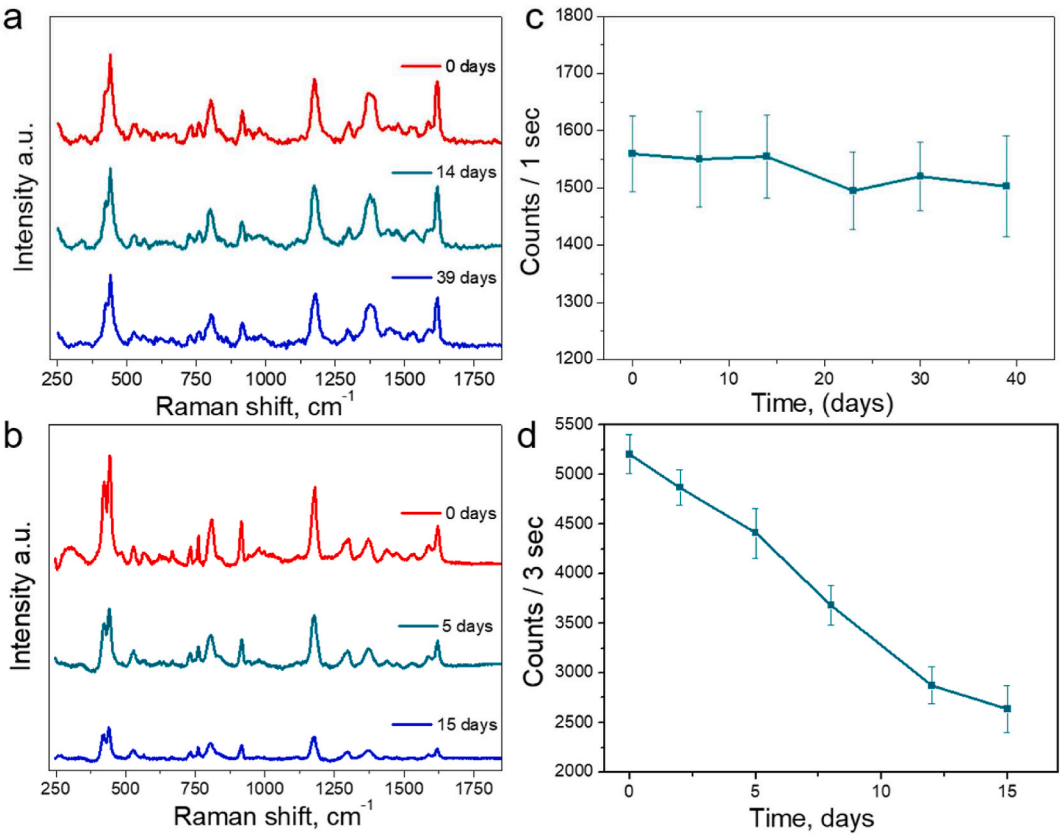

Fig. 6. Time-dependent SERS spectra of the CV with the concentration of 10^{-6} M obtained from the NPs formed by a) ion-beam irradiation method, b) annealing method, intensity of 443 cm^{-1} Raman band on the days after the fabrication NPs by ion-beam irradiation (c) and annealing (d) methods consistently.

irradiation method. The following relation is used:

$$EF = \frac{I_{SERS}}{I_{ref}} \frac{C_{ref}}{C_{SERS}} \quad (1)$$

where I_{SERS} and I_{ref} represent background-subtracted intensities of the 443 cm^{-1} band for the CV adsorbed on the glass substrates and glass substrates with Ag NPs. C_{SERS} and C_{ref} represent the corresponding concentrations of the CV on the glass substrates and glass substrates with Ag NPs. The estimated average EF of the NPs formed by ion irradiation is $\sim 0.8 \times 10^5$ and $\sim 1.3 \times 10^5$ for the ones formed by the annealing consequently. The enhancement factor is more or less typical for silver nanoparticles having a spheroidal shape [41]. However, the comparison between the EF of current samples and other structures is hindered by the 532 nm excitation wavelength proximity to the absorbance band of CV. Prominent absorbance of exciting radiation ensures resonant Raman scattering conditions, thus leading to surface-enhanced resonant Raman scattering manifestation. We should also note that amplification factor for the annealed particles is slightly larger, which can be attributed to their size and areal density being higher than those of the ion-irradiated NPs. Such morphological features of the annealed structures lead to a higher concentration of their SERS hotspots [42], which apparently enhances the EF of the annealed films in comparison to the irradiated ones. At the current stage, we presented and discussed the stability of the obtained nanoparticles; the subsequent optimization of the parameters of the suggested technique will be carried out to increase the enhancement factor of the structure.

4. Conclusions

In conclusion, we have demonstrated that the technology of ion-beam modification makes it possible to create monocrystalline silver nanoparticles and to ensure the nanostructuring of complex surfaces. Using high resolution TEM images, XPS analysis and SERS spectroscopy, we have unambiguously shown that Ag NPs having a monocrystalline structure are resistant to oxidation compared to NPs having a polycrystalline structure. The high SERS amplification factor, persisting for more than one month of storage in the ambient atmosphere, demonstrates their higher efficiency compared to the polycrystalline Ag NPs, which lose efficiency even five days after their manufacturing. Thus, we have demonstrated a new approach to the fabrication of single-crystal Ag NPs, featuring high stability of their plasmonic properties and the possibility of nanostructuring both large areas and complex surfaces by the combination of electron lithography and ion-beam-irradiation methods. We suppose the presented results to be of high interest for the various applications which require dynamic Raman measurements with high sensitivity, for example, *in situ* analysis of biological processes or chemical reactions and the assessment of compounds degradation and stability.

Funding sources

We gratefully acknowledge the financial support from the Ministry of Science and Higher Education of the Russian Federation (Agreement No. 075-15-2022-1150). V.B. acknowledges the support of the Latvian Council of Science (project: "DNSSN", No. lzp-2021/1–0048). S.M.N. and I.A.Z. acknowledge the financial support from Ministry of Science and Higher Education of the Russian Federation (No. FSMG-2024-0014). The work for the synthesis of a SERS-active surface was financially supported by RSF (grant N°23-13-00276).

CRediT authorship contribution statement

Natalia V. Doroshina: Writing – original draft, Investigation. **Oleg A. Streletskiy:** Writing – review & editing, Investigation, Conceptualization. **Ilya A. Zavidovskiy:** Writing – original draft, Methodology, Data curation. **Mikhail K. Tatmyshevskiy:** Writing – review & editing, Investigation. **Gleb I. Tselikov:** Writing – review & editing, Investigation, Data curation. **Olesya O. Kapitanova:** Investigation. **Alexander V. Syuy:** Investigation. **Roman Romanov:** Investigation, Data curation. **Prabhash Mishra:** Methodology, Investigation. **Vjaceslavs Bobrovs:** Writing – review & editing, Investigation, Formal analysis. **Andrey M. Markeev:** Writing – review & editing, Investigation, Formal analysis. **Dmitry I. Yakubovsky:** Writing – review & editing, Investigation. **Irina A. Veselova:** Writing – review & editing, Investigation, Data curation. **Aleksey V. Arsenin:** Writing – review & editing, Investigation, Formal analysis. **Valentyn S. Volkov:** Writing – review & editing, Methodology, Investigation, Data curation. **Sergey M. Novikov:** Writing – review & editing, Supervision, Project administration, Conceptualization.

Declaration of competing interest

The authors declare that they have no known competing financial interests or personal relationships that could have appeared to influence the work reported in this paper.

Acknowledgments

We express our gratitude to Ivanenko I.P and Ozerova K.E. The research was carried out using the equipment of MSU Shared Research Equipment Center “Technologies for obtaining new nanostructured materials and their complex study” and purchased by MSU in the frame of the Equipment Renovation Program (National Project “Science”) and in the frame of the MSU Program of

Development.

Appendix A. Supplementary data

Supplementary data to this article can be found online at https://doi.org/10.1016/j.heliyon.2024.e27538.

References

[1] D.K. Gramotnev, S.I. Bozhevolnyi, Plasmonics beyond the diffraction limit, Nat. Photonics 4 (2010) 83–91, https://doi.org/10.1038/nphoton.2009.282.
[2] A.V. Krasavin, P. Ginzburg, G.A. Wurtz, A.V. Zayats, Nonlocality-driven supercontinuum white light generation in plasmonic nanostructures, Nat. Commun. 7 (2016) 11497, https://doi.org/10.1038/ncomms11497.
[3] J.A. Schuller, E.S. Barnard, W. Cai, Y.C. Jun, J.S. White, M.L. Brongersma, Plasmonics for extreme light concentration and manipulation, Nat. Mater. 9 (2010) 193–204, https://doi.org/10.1038/nmat2630.
[4] S. Lal, S. Link, N.J. Halas, Nano-optics from sensing to waveguiding, Nat. Photonics 1 (2007) 641–648, https://doi.org/10.1038/nphoton.2007.223.
[5] A.B. Evlyukhin, A.I. Kuznetsov, S.M. Novikov, J. Beermann, C. Reinhardt, R. Kiyan, S.I. Bozhevolnyi, B.N. Chichkov, Optical properties of spherical gold mesoparticles, Appl. Phys. B 106 (2012) 841–848, https://doi.org/10.1007/s00340-011-4727-5.
[6] S.A. Maier, Plasmonics: Fundamentals and Applications, Springer, New York, 2007.
[7] J. Langer, D. Jimenez de Aberasturi, J. Aizpurua, R.A. Alvarez-Puebla, B. Auguié, J.J. Baumberg, G.C. Bazan, S.E.J. Bell, A. Boisen, et al., Present and future of surface-enhanced Raman scattering, ACS Nano 14 (2020) 28–117, https://doi.org/10.1021/acsnano.9b04224.
[8] J. Beermann, S.M. Novikov, O. Albrektsen, M.G. Nielsen, S.I. Bozhevolnyi, Surface-enhanced Raman imaging of fractal shaped periodic metal nanostructures, J. Opt. Soc. Am. B, JOSAB 26 (2009) 2370–2376, https://doi.org/10.1364/JOSAB.26.002370.
[9] A. Buccolieri, S. Bettini, L. Salvatore, F. Baldassarre, G. Ciccarella, G. Giancane, Sub-nanomolar detection of biogenic amines by SERS effect induced by hairy Janus silver nanoparticles, Sensor. Actuator. B Chem. 267 (2018) 265–271, https://doi.org/10.1016/j.snb.2018.04.028.
[10] K. Kneipp, Y. Wang, H. Kneipp, L.T. Perelman, I. Itzkan, R.R. Dasari, M.S. Feld, Single molecule detection using surface-enhanced Raman scattering (SERS), Phys. Rev. Lett. 78 (1997) 1667–1670, https://doi.org/10.1103/PhysRevLett.78.1667.
[11] N.L. Gruenke, M.F. Cardinal, M.O. McAnally, R.R. Frontiera, G.C. Schatz, R.P.V. Duyne, Ultrafast and nonlinear surface-enhanced Raman spectroscopy, Chem. Soc. Rev. 45 (2016) 2263–2290, https://doi.org/10.1039/C5CS00763A.
[12] S.M. Novikov, S. Boroviks, A.B. Evlyukhin, D.E. Tatarkin, A.V. Arsenin, V.S. Volkov, S.I. Bozhevolnyi, Fractal shaped periodic metal nanostructures atop dielectric-metal substrates for SERS applications, ACS Photonics 7 (2020) 1708–1715, https://doi.org/10.1021/acsphotonics.0c00257.
[13] Z. Chen, X. Su, H. Luo, A. Ade, H. Zhu, Y. Zhang, L. Yu, Transparent conductive film of silver nanowires employed for SERS detection of mercury ions, Mater. Chem. Phys. 309 (2023) 128335, https://doi.org/10.1016/j.matchemphys.2023.128335.
[14] K.-Q. Lin, J. Yi, J.-H. Zhong, S. Hu, B.-J. Liu, J.-Y. Liu, C. Zong, Z.-C. Lei, X. Wang, J. Aizpurua, R. Esteban, B. Ren, Plasmonic photoluminescence for recovering native chemical information from surface-enhanced Raman scattering, Nat. Commun. 8 (2017) 14891, https://doi.org/10.1038/ncomms14891.
[15] S. Vishnupriya, K. Chaudhari, R. Jagannathan, T. Pradeep, Single-cell investigations of silver nanoparticle–bacteria interactions, Part. Part. Syst. Char. 30 (2013) 1056–1062, https://doi.org/10.1002/ppsc.201300165.
[16] T.M. Machado, L.P.F. Peixoto, G.F.S. Andrade, M.A.P. Silva, Copper nanoparticles–containing tellurite glasses: an efficient SERS substrate, Mater. Chem. Phys. 278 (2022) 125597, https://doi.org/10.1016/j.matchemphys.2021.125597.
[17] N.A. Brazhe, E.I. Nikelshparg, A.A. Baizhumanov, V.G. Grivennikova, A.A. Semenova, S.M. Novikov, V.S. Volkov, A.V. Arsenin, D.I. Yakubovsky, A. B. Evlyukhin, Z.V. Bochkova, E.A. Goodilin, G.V. Maksimov, O. Sosnovtseva, A.B. Rubin, SERS uncovers the link between conformation of cytochrome c heme and mitochondrial membrane potential, Free Radic. Biol. Med. 196 (2023) 133–144, https://doi.org/10.1016/j.freeradbiomed.2023.01.013.
[18] X.K. Meng, S.C. Tang, S. Vongehr, A review on diverse silver nanostructures, J. Mater. Sci. Technol. 26 (2010) 487–522, https://doi.org/10.1016/S1005-0302(10)60078-3.
[19] I. Pastoriza-Santos, L.M. Liz-Marzán, Colloidal silver nanoplates. State of the art and future challenges, J. Mater. Chem. 18 (2008) 1724–1737, https://doi.org/10.1039/B716538B.
[20] C.D. Sai, Q.H. Nguyen, T.N.A. Tran, V.T. Pham, T.B. Nguyen, H.H. Do, T.D. Vu, CuO nanorods decorated gold nanostructures as an ultra-sensitive and recyclable SERS substrate, Mater. Chem. Phys. 293 (2023) 126962, https://doi.org/10.1016/j.matchemphys.2022.126962.
[21] X. Zhang, E.M. Hicks, J. Zhao, G.C. Schatz, R.P. Van Duyne, Electrochemical tuning of silver nanoparticles fabricated by nanosphere lithography, Nano Lett. 5 (2005) 1503–1507, https://doi.org/10.1021/nl050873x.
[22] W. Cao, H.E. Elsayed-Ali, Stability of Ag nanoparticles fabricated by electron beam lithography, Mater. Lett. 63 (2009) 2263–2266, https://doi.org/10.1016/j.matlet.2009.07.052.
[23] Z.-L. Song, Z. Chen, X. Bian, L.-Y. Zhou, D. Ding, H. Liang, Y.-X. Zou, S.-S. Wang, L. Chen, C. Yang, X.-B. Zhang, W. Tan, Alkyne-functionalized superstable graphitic silver nanoparticles for Raman imaging, J. Am. Chem. Soc. 136 (2014) 13558–13561, https://doi.org/10.1021/ja507368z.
[24] A. Gutés, R. Maboudian, C. Carraro, Gold-coated silver dendrites as SERS substrates with an improved lifetime, Langmuir 28 (2012) 17846–17850, https://doi.org/10.1021/la303421s.
[25] S.M. Novikov, V.N. Popok, A.B. Evlyukhin, M. Hanif, P. Morgen, J. Fiutowski, J. Beermann, H.-G. Rubahn, S.I. Bozhevolnyi, Highly stable monocrystalline silver clusters for plasmonic applications, Langmuir 33 (2017) 6062–6070, https://doi.org/10.1021/acs.langmuir.7b00772.
[26] M. Hanif, R.R. Juluri, M. Chirumamilla, V.N. Popok, Poly(methyl methacrylate) composites with size-selected silver nanoparticles fabricated using cluster beam technique, J. Polym. Sci. B Polym. Phys. 54 (2016) 1152–1159, https://doi.org/10.1002/polb.24021.
[27] M. Hanif, V.N. Popok, Magnetron sputtering cluster apparatus for formation and deposition of size-selected metal nanoparticles, in: Physics, Chemistry and Applications of Nanostructures, WORLD SCIENTIFIC, 2015, pp. 416–419, https://doi.org/10.1142/9789814696524_0103.
[28] V.N. Popok, Formation and applications of polymer films with gas-phase aggregated nanoparticles: a brief review, Thin Solid Films 756 (2022) 139359, https://doi.org/10.1016/j.tsf.2022.139359.
[29] H. Hartmann, V.N. Popok, I. Barke, V. von Oeynhausen, K.-H. Meiwes-Broer, Design and capabilities of an experimental setup based on magnetron sputtering for formation and deposition of size-selected metal clusters on ultra-clean surfaces, Rev. Sci. Instrum. 83 (2012) 073304, https://doi.org/10.1063/1.4732821.
[30] O. Streletskiy, I. Zavidovskiy, D. Yakubovsky, N. Doroshina, A. Syuy, Y. Lebedinskij, A. Markeev, A. Arsenin, V. Volkov, S. Novikov, Tailoring of the distribution of SERS-active silver nanoparticles by post-deposition low-energy ion beam irradiation, Materials 15 (2022) 7721, https://doi.org/10.3390/ma15217721.
[31] A.E.B. Presland, G.L. Price, D.L. Trimm, Hillock formation by surface diffusion on thin silver films, Surf. Sci. 29 (1972) 424–434, https://doi.org/10.1016/0039-6028(72)90229-4.
[32] F. Baletto, R. Ferrando, Structural properties of nanoclusters: energetic, thermodynamic, and kinetic effects, Rev. Mod. Phys. 77 (2005) 371–423, https://doi.org/10.1103/RevModPhys.77.371.
[33] W. Bock, H. Gnaser, H. Oechsner, Modification of crystalline semiconductor surfaces by low-energy Ar+ bombardment: Si(111) and Ge(100), Surf. Sci. 282 (1993) 333–341, https://doi.org/10.1016/0039-6028(93)90938-G.
[34] S. Hans, M. Ranjan, Emergence of triangular features on ion irradiated silicon (100) surface, Surf. Sci. 715 (2022) 121951, https://doi.org/10.1016/j.susc.2021.121951.

[35] W.M. Haynes, CRC Handbook of Chemistry and Physics, CRC Press, 2014.
[36] S.W. Gaarenstroom, N. Winograd, Initial and final state effects in the ESCA spectra of cadmium and silver oxides, J. Chem. Phys. 67 (2008) 3500–3506, https://doi.org/10.1063/1.435347.
[37] Y. Han, R. Lupitskyy, T.-M. Chou, C.M. Stafford, H. Du, S. Sukhishvili, Effect of oxidation on surface-enhanced Raman scattering activity of silver nanoparticles: a quantitative correlation, Anal. Chem. 83 (2011) 5873–5880, https://doi.org/10.1021/ac2005839.
[38] E.Z. Luo, S. Heun, M. Kennedy, J. Wollschläger, M. Henzler, Surface roughness and conductivity of thin Ag films, Phys. Rev. B 49 (1994) 4858–4865, https://doi.org/10.1103/PhysRevB.49.4858.
[39] S. Fateixa, H.I.S. Nogueira, T. Trindade, Surface-enhanced Raman scattering spectral imaging for the attomolar range detection of crystal violet in contaminated water, ACS Omega 3 (2018) 4331–4341, https://doi.org/10.1021/acsomega.7b01983.
[40] E.C. Le Ru, E. Blackie, M. Meyer, P.G. Etchegoin, Surface enhanced Raman scattering enhancement factors: a comprehensive study, J. Phys. Chem. C 111 (2007) 13794–13803, https://doi.org/10.1021/jp0687908.
[41] D.M. Solís, J.M. Taboada, F. Obelleiro, L.M. Liz-Marzán, F.J. García de Abajo, Optimization of nanoparticle-based SERS substrates through large-scale realistic simulations, ACS Photonics 4 (2017) 329–337, https://doi.org/10.1021/acsphotonics.6b00786.
[42] E. Babich, S. Scherbak, F. Asonkeng, T. Maurer, A. Lipovskii, Hot spot statistics and SERS performance of self-assembled silver nanoisland films, Opt. Mater. Express, OME 9 (2019) 4090–4096, https://doi.org/10.1364/OME.9.004090.